International Journal of Technology (2017) 4: 582-590
ISSN 2086-9614

SYNTHESIS AND CHARACTERIZATION OF HEMATITE NANOPARTICLES USING ULTRASONIC SONOCHEMISTRY METHOD

Munawar Khalil[1*], Ning Liu[2], Robert L. Lee[3]

[1]*Department of Chemistry, Faculty of Mathematics and Natural Science, Universitas Indonesia, Kampus UI Depok, Depok 16424, Indonesia*
[2]*Department of Petroleum Engineering, University of Lousiana at Lafayette, 70504 Lousiana, USA*
[3]*Petroleum Recovery Research Center (PRRC), New Mexico Tech, 87801 Socorro, NM, USA*

(Received: January 2017 / Revised: May 2017 / Accepted: June 2017)

ABSTRACT

This paper presents an investigation on the method for synthesizing hematite nanoparticle using ultrasonic sonochemistry. The effect of various bases with different basicity strengths, i.e. NaOH, NH_4OH, and butylamine, as well as sintering treatment on the purity and crystallinity of hematite nanoparticles was studied. In this work, the as-synthesized hematite nanoparticles were characterized using FTIR, XRD, and HR-TEM analyses. The results showed that the formation of hematite crystal can undergo two possible reaction pathways depending on the basicity of the solution. When strong bases like NaOH and butylamine were used, iron(III) ion could react with water to form iron complexes, which further grow into rod-like magnetite nanocrystals as the major product. However, direct reaction of iron(III) ion with hydroxide ion to form hematite was observed when a weak base like NH_4OH was used. Furthermore, it was also found that most of the polymorphous iron oxide precursors can be transformed into hematite crystals via high-temperature sintering.

Keywords: Hematite; Iron oxide; Nanoparticles; Sintering; Ultrasonic sonochemistry

1. INTRODUCTION

Research on the synthesis of various forms of iron oxide nanoparticles has increased considerably over the past decades because of the vast and remarkable potential of iron oxide nanoparticles for many applications. Because of their unique physical and chemical properties, iron oxide nanoparticles are readily used in various applications such as in catalysis, diagnostic imaging, drug delivery, electrodes in non-aqueous batteries, and catalysts (Khalil et al., 2017; Hassanjani-Roshan et al., 2011; Kulkarni & Lokhande, 2003; Sha et al., 2004; Lee et al., 2009; Caudron et al., 2011; Lu et al., 2012; Tadić et al., 2011). In recent years, studies on the development of simple and robust methods for synthesizing iron oxide nanoparticles has attracted considerable interest, especially in the area of nanotechnology (Tadić et al., 2011, Caudron et al., 2011; Lu et al., 2012). Among the different crystal forms of iron oxide, hematite (α-Fe_2O_3) has been the focus of several studies interests because of its high stability, high resistance to corrosion, low cost, environment friendliness, and non-toxicity (Tadić et al., 2011).

Various methods for synthesizing nanosized hematite particles, such as sol-gel, co-precipitation, and hydrothermal methods, have been widely reported (Davar et al., 2016;

*Corresponding author's email: mkhalil@sci.ui.ac.id, Tel. +62-21-7270027, Fax. +62-21- 7863432
Permalink/DOI: https://doi.org/10.14716/ijtech.v8i4.7285

Cuong et al., 2014; Khalil et al., 2014). However, synthetic methods that allow large-scale production with precise control of the size, morphology and dispersity are still underdeveloped. Recently, the synthesis of hematite nanoparticles using an ultrasonic sonochemistry method has been considered as an easy and robust way to fabricate uniform nanosized hematite crystals from different types of iron sources (Hassanjani-Roshan et al., 2011). The synthesis of hematite nanoparticles via ultrasonic sonochemistry is mostly carried out using $Fe(CO)_5$ as the iron source (Bang & Suslick, 2007). However, recent studies reported that different types of iron precursors, such as $Fe(acac)_3$ (Pinkas et al., 2008), $FeCl_3$ (Hassanjani-Roshan et al., 2011; Kim et al., 2007), $Fe(NO)_3$ (Schmidt, 2001) and $Fe(OAc)_2$ (Vijaykumar et al., 2001), could also be used. This is because of the ability of ultrasonic irradiation to cause cavitation in an aqueous medium that generates high temperature and pressure, which result in many unusual chemical reactions (Ashokkumar et al., 2007; Suslick, 1998; Wang et al., 2003). Therefore, the development of a concise and robust route for synthesizing hematite nanoparticles via ultrasonic sonochemistry method is presented in this work. The main objective of this work is to provide a comprehensive understanding towards the formation of nanosized hematite crystals under ultrasonic irradiation.

2. EXPERIMENTAL METHODS

To synthesize hematite nanoparticles, 0.3 M $FeCl_3.6H_2O$ (Alfa Aesar) aqueous solution was first made and added in a dropwise manner to 0.1 M aqueous solution of each of the bases, i.e. NaOH (K_b = 8.51), NH_4OH ($K_b = 1.78\times10^{-5}$), and butylamine ($K_b = 5.9\times10^{-4}$) (purchased from Sigma-Aldrich) under the influence of 80% amplitude of ultrasonic irradiation (Q-sonicator Model Q500, Misonix Sonicator) for 45 min. After the reaction, the mixture was then evaporated, and the red precipitate was mashed and divided into two separate samples. The first sample was directly characterized using Fourier transform infrared spectroscopy (FTIR; Thermo Nicolet Avatar 360 FTIR Spectrometer instrument), X-ray diffraction (XRD; SIEMENS D500 Bruker with Cu Kα radiation source), and high-resolution transmission electron microscopy (HR-TEM; JEOL 2010 EX) with an Oxford-Link energy-dispersive X-ray spectroscope (EDS) and a Gatan digital micrograph equipped with slow scan charge coupled device (CCD) camera and operated at 200 kV. Meanwhile, the second sample was treated under a sintering process at 500°C for 1 h before being characterized by similar analyses. The overall schematic diagram for the synthesis method is presented in Figure 1.

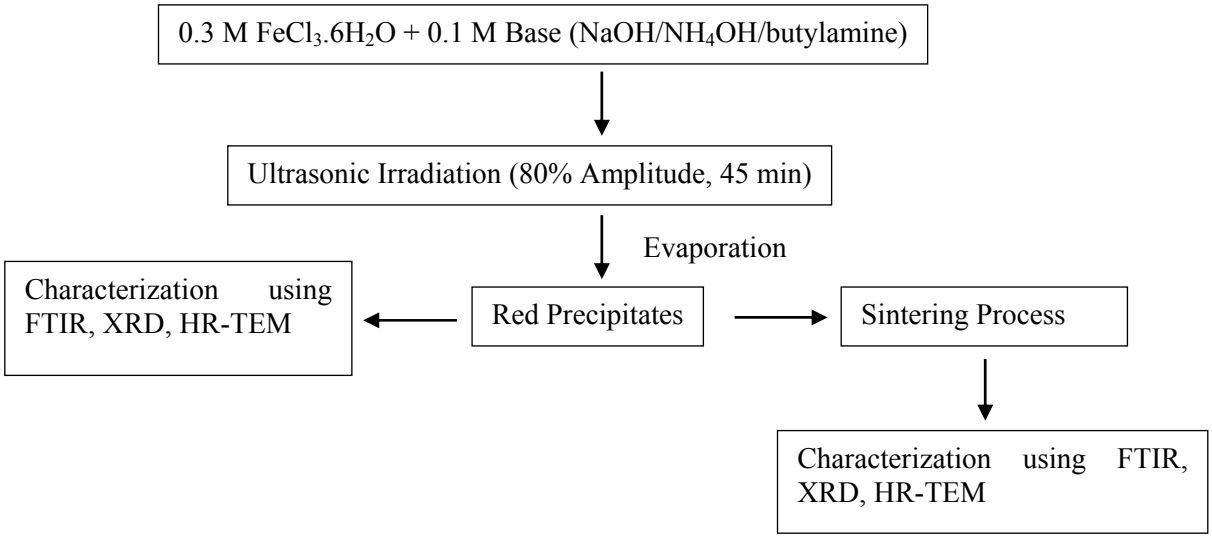

Figure 1 Schematic diagram of the synthesis method of hematite nanoparticles

3. RESULTS AND DISCUSSION

3.1. Effect of Basicity

Figure 2 presents FTIR spectra for the reaction products synthesized using different types of bases prior to the sintering process. In the literature, any type of iron oxide crystalline phase can be identified with IR absorption band for the Fe-O stretch vibrations and Fe-OH bending vibrations at approximately around 565.6 and 479.7 cm^{-1}, respectively (Lu et al., 2012; Rendon & Serna, 1981). Based on the results, almost all reaction products obtained after the evaporation process strongly absorbed IR at these two wave numbers with a slight shift that occurred as a result of quantum confinement, size, dipolar interaction, surface amorphousness, particle aggregation, or interfacial effects (Chernyshova et al., 2007). Broad spectra and the appearance of unnecessary peaks at higher wavenumbers (>1000 s^{-1}) are assumed to be the result of impurities. For instance, a sharp peak at around 3200 cm^{-1} and 1600 cm^{-1} for the amine N-H was observed in the reaction products synthesized using NH_4OH and butylamine (Figures 2b and 2c). However, these peaks were absent for the reaction product synthesized with NaOH (Figure 2a). This is mainly the result of absorption of unreacted NH_3 and/or butylamine on the surface of the iron oxide crystals. Moreover, a sharp peak was observed at ~2900 cm^{-1} owing to the presence of an alkyl chain of C-H in the reaction product from butylamine. In addition, a broad peak for OH stretch around 3300 cm^{-1} was also observed.

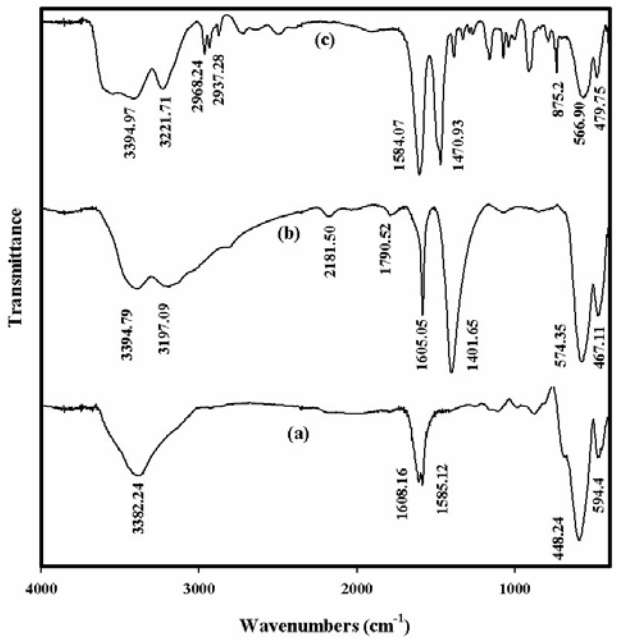

Figure 2 FTIR spectra of reaction products synthesized using: (a) NaOH; (b) NH_4OH; and (c) butylamine

Figure 3 presents the XRD pattern of the reaction products obtained from the evaporation process after ultrasonic irradiation using different types of bases. The XRD results demonstrate that the reaction products obtained after evaporation process were composed of three different crystal types of iron oxides, namely magnetite (Fe_3O_4), geothite (α-FeOOH), and hematite (α-Fe_2O_3), depending on the type of base used in the reaction. For reaction products obtained using a stronger base like NaOH or butylamine, the XRD patterns are mostly dominated by peaks assigned for magnetite and geothite (Figures 3a and 3c). Specific peaks for the hematite crystal were either very weak or absent. This suggests that the ultrasonic sonochemistry reaction of an iron salt and base with high degree of basicity such as NaOH and butylamine would more likely produce a mixture of geothite and magnetite crystal instead of hematite. However, result

suggests that direct hematite production could be achieved when a weak base like NH_4OH was used as the precursor. This is proven by the appearance of specific peaks for the hematite crystal in the XRD pattern of the reaction product when using NH_4OH (Figure 3b).

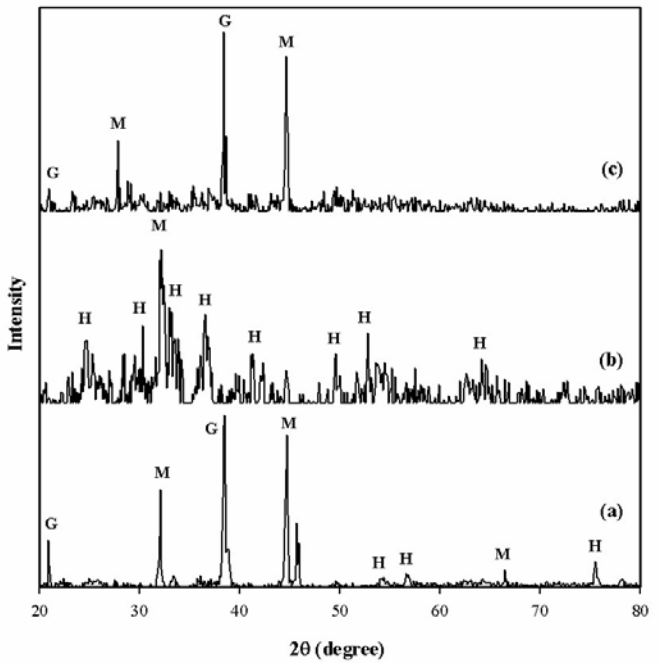

Figure 3 XRD pattern of reaction products synthesized using: (a) NaOH; (b) NH_4OH; and (c) butylamine (H: hematite, G: geothite, M: magnetite)

Figure 4 presents HRTEM images of the reaction products synthesized using bases with different basicity values. The results reveal that the reaction products are dominated with uniform monodisperse rod-like nanoparticles, especially for the reaction products synthesized using NaOH and NH_4OH (Figures 4a and 4b). Synthesis using NaOH would render slightly bigger particles than when using NH_4OH even though the particles shared similar a particle shape and morphology. This is most likely because of different rates in particle growth owing to the different strengths of basicity. It appears that a strong base like NaOH can increase the rate of particle growth of the crystal by providing high amount of hydroxide ions for hydrolysis of iron salt to form iron oxide crystal. As the result, more crystal seeds are generated that further grow into larger crystal particles. Furthermore, a mixture between rod-like particles and very small sphere-like particles, which severely aggregated to form big nanoparticles clusters, was observed for the reaction product synthesized using butylamine (Figure 4c). This severe aggregation is mostly due to the hydrophobic and van der Waals interactions of unreacted butylamine absorbed on the surface of the nanoparticles.

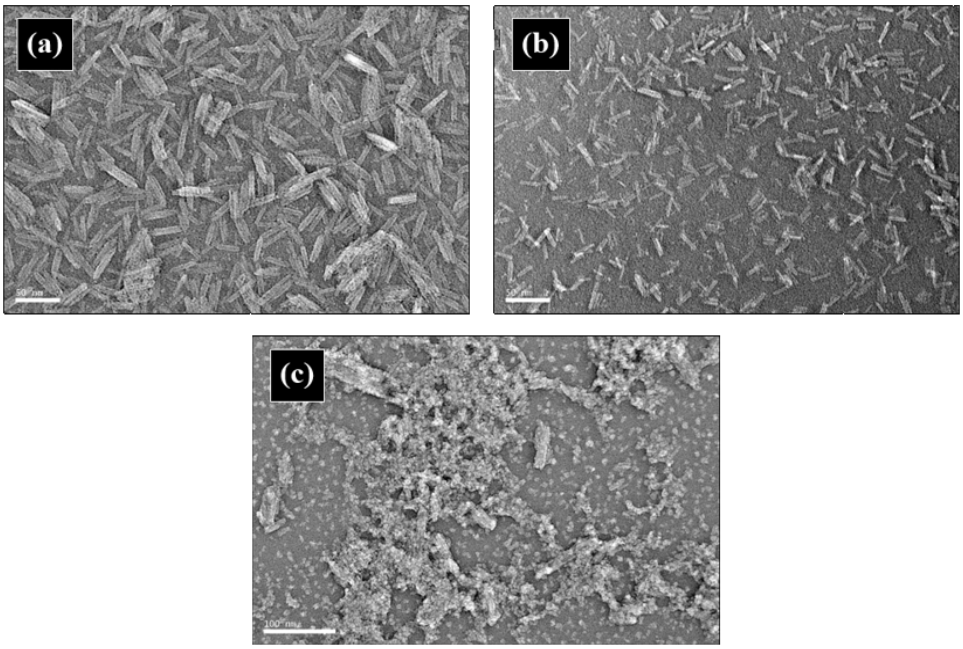

Figure 4 HRTEM images of reaction products synthesized using: (a) NaOH; (b) NH_4OH; and (c) butylamine

3.2. Effect of Sintering

In this work, the sintering process was carried out at 500°C for reaction products synthesized using different types of bases under the influence of ultrasonic irradiation. The objectives of this process are to eliminate the presence of impurities and to improve the crystallinity of the hematite crystals. Figure 5 shows the FTIR spectra of the sintered reaction products synthesized using different types of bases. The results indicate that the sintering process eliminated most of the impurities. The appearance of unnecessary peaks at higher wavenumbers seen in the reaction products without sintering was effectively reduced or even eliminated after sintering. It is believed that, at high temperatures, impurities such as unreacted reactants and by products were destroyed during the sintering process.

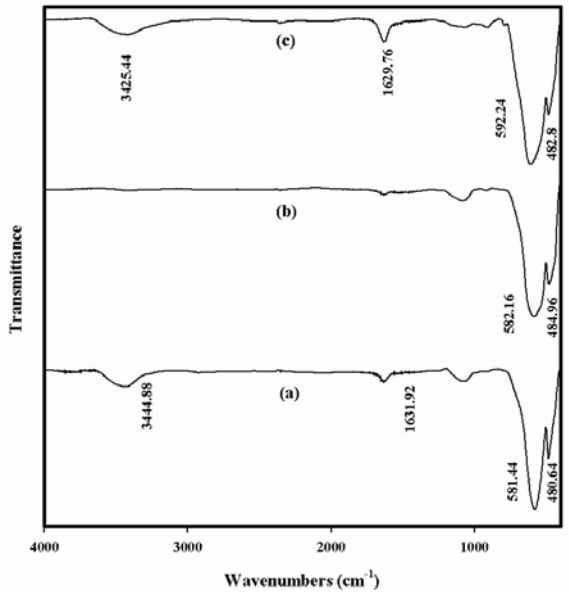

Figure 5 FTIR spectra of sintered reaction products synthesized using: (a) NaOH; (b) NH_4OH; and (c) butylamine

The XRD results also suggested that other types of polymorphous iron oxides, i.e. magnetite and goethite, could be transformed into hematite through the sintering process at high temperatures (Figure 6). Nevertheless, specific peaks for magnetite and geothite were still observed, especially in reaction products synthesized using stronger bases like NaOH and butylamine, owing to the incomplete crystal phase transformation. However, for NH_4OH reaction products, the XRD pattern clearly shows the presence of hematite without any sign of impurities, suggesting that pure hematite crystals were formed under this condition. In addition, the crystal size of this reaction product, calculated using Debye–Scherrer's approximation (Equation 1), was found to be approximately around 13.7 nm.

$$D = \frac{k\lambda}{\beta \cos\theta} \tag{1}$$

where D is the crystalline size (nm), k is a grain shape dependent constant (assumed to be 0.89 for spherical particles), λ is the wavelength of the X-ray beam (0.15406 nm for the Cu Kα radiation), β is the full width at half maximum for the diffraction peak (in radians), and θ is the diffraction angle (33.4° for the rhombohedral α-Fe_2O_3 reflected at (104) plane).

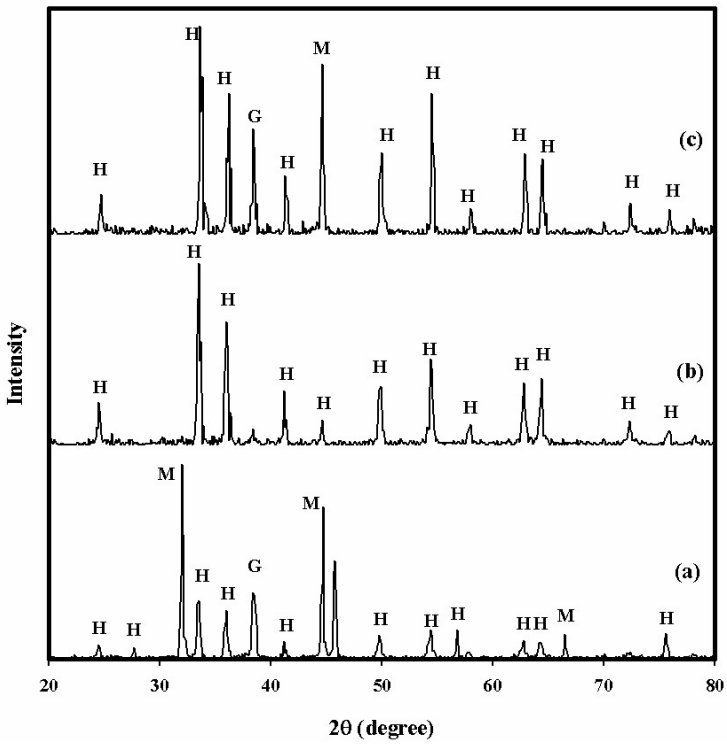

Figure 6 XRD pattern of sintered reaction products synthesized: (a) NaOH; (b) NH_4OH; and (c) butylamine (H: hematite, G: geothite, M: magnetite)

Further analysis using HRTEM also revealed that polyhedron nanosized particles could be obtained from the sintering process (Figure 7). Results demonstrated that considerably large polyhedron nanoparticles with multi-dispersity were obtained when strong bases like NaOH and butylamine were used in the reaction. In addition, rod-like nanoparticles, which were assumed to be remaining magnetite and geothite nanocrystals, were still observed. This result is also supported by XRD analysis where specific peaks for magnetite and geothite still appeared among the hematite peaks (Figures 6a and 6c). Conversely, monodispersed polyhedron nanoparticles with particle size of around 14 nm, which according to XRD data were believed

to be the hematite crystals, were obtained when NH_4OH was used (Figure 7b).

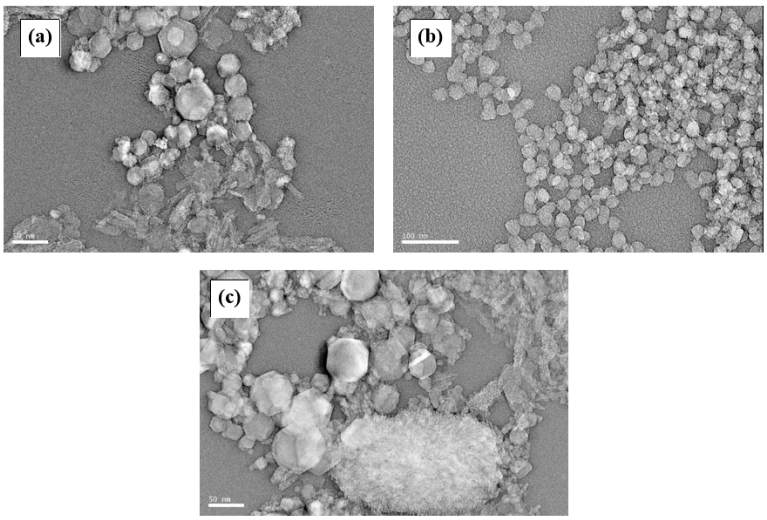

Figure 7 HRTEM images of sintered reaction products synthesized using: (a) NaOH; (b) NH_4OH; and (c) butylamine

3.3. Growth Mechanism

In general, hematite crystals can form a dissociation of iron salt in water at basic conditions (Hassanjani-Roshan et al., 2011). The formation of hematite crystals is initiated by the formation of iron hydroxide ($Fe(OH)_3$), which can be further converted to geothite (α-FeOOH) crystals. Under ultrasonic irradiation, geothite crystals can further undergo phase transformation to form hematite crystals by releasing water as a by product. However, iron(III) ions could sometimes form a stable molecular complex species with water. Instead of forming $Fe(OH)_3$, iron(III) could form an octahedral complex species of hexaaquairon(III) ion ($[Fe(H_2O)_6]^{3+}$), which under ultrasonic irradiation could further transform into pentaaquahydroxyiron(III) ion ($[Fe(H_2O)_5(OH)]^{2+}$) where one of the water ligand is replaced by a hydroxide ion. When a strong base like NaOH or butylamine is added to the solution, ($[Fe(H_2O)_5(OH)]^{2+}$) could further be converted into tetraaquadihydroxyiron(III) ion ($[Fe(H_2O)_4(OH)_2]^{+}$) by replacing one more water ligand with hydroxide ion and reduces the iron oxidation state from 3 to 2. As a result, the amount of iron(II) ions in the solution is increased and may lead to the formation of $Fe(OH)_2$, which favors the formation of magnetite (Fe_3O_4).

Based on the aforementioned data, it is possible that the nanosized hematite crystals obtained in this work were formed via both reaction pathways depending on the strength of the bases. When a weak base like NH_4OH was used, direct reaction of iron(III) ion with hydroxide to initially form geothite and further transform into hematite is more dominant. Meanwhile, when strong bases such as NaOH and butylamine were used, both reaction pathways could occur. However, the formation of iron complexes, which lead to the formation of magnetite, was found to be more favorable. This is proven by the superiority of specific peaks for magnetite intensity compared to specific peaks for both geothite and hematite. Nevertheless, these rod-like magnetite crystals were mostly transformed into polyhedron hematite nanoparticles at high temperature owing to the sintering process.

4. CONCLUSION

Three different types of bases, i.e. NaOH, NH_4OH, and butylamine, with different strengths of basicity have been successfully used in ultrasonic sonochemistry method to synthesize hematite nanoparticles. Based on the results, it is believed that there are two possible key reaction

pathways that are responsible for the formation of hematite crystals depending on the basic strength of the basicity of the reaction precursors. When strong bases like NaOH and butylamine were used, the formation of hematite was dominated by the formation of iron complexes and the formation of magnetite which ultimately transforms into hematite during the sintering process. Meanwhile, when a weak base like NH_4OH was used, direct reaction of iron(III) ion with a hydroxide to initially form geothite and ultimately transform into hematite was found to be the most predominant process. This was proved by FTIR, XRD, and HR-TEM analyses. Based on the results, uniform monodisperse polyhedron hematite nanoparticles with particle size of around 14 nm could be obtained when NH_4OH was used in the ultrasonic sonochemistry followed by sintering process at 500°C.

5. ACKNOWLEDGEMENT

We gratefully acknowledge the financial support of the US Department of Energy through the National Energy Technology Laboratory under contract number DE-FE0005979.

6. REFERENCES

Ashokkumar, M., Lee, J., Kentish, S., Grieser, F., 2007. Bubbles in an Acoustic Field: An Overview. *Ultrasonics Sonochemistry*, Volume 14, pp. 470–475

Bang, J.H., Suslick, K.S., 2007. Sonochemical Synthesis of Nanosized Hollow Hematite. *Journal of the American Chemical Society*, Volume 129, pp. 2242–2243

Caudron, E., Tfayli, A., Monnier, C., Manfait, M., Prognon, P., Pradeau, D., 2011. Identification of Hematite Particles in Sealed Glass Containers for Pharmaceutical Uses by Raman Microspectroscopy. *Journal of Pharmaceutical and Biomedical Analysis*, Volume 54, pp. 866–868

Chernyshova, I.V., Hochella Jr., M.F., Madden, A.S., 2007. Size-dependent Structural Transformation of Hematite Nanoparticles. 1. Phase Transition. *Physical Chemistry Chemical Physics*, Volume 9, pp. 1736–1750

Cuong, N.Y., Hoa, T.T., Khieu, D.Q., Hoa, N.D., Hieu, N.V., 2012. Gas Sensor based on Nanoporous Hematite Nanoparticles: Effect of Synthesis Pathways on Morphology and Gas Sensing Properties. *Current Applied Physics*, Volume 12(5), pp. 1355–1360

Davar, F., Hadadzadeh, H., Alaedini, T.S., 2016. Single-phase Hematite Nanoparticles: Non-alkoxide Sol-gel based Preparation, Modification and Characterization. *Ceramics International*, Volume 42(16), pp. 19336–19342

Hassanjani-Roshan, A., Vaezi, M.R., Shokuhfar, A., Rajabali, Z. 2011. Synthesis of Iron Oxide Nanoparticles via Sonochemical Method and their Characterization. *Particuology*, Volume 9, pp. 95–99

Khalil, M., Yu, J., Liu, N., Lee, R.L., 2014. Hydrothermal Synthesis, Characterization, and Growth Mechanism of Hematite Nanoparticles. *Journal of Nanoparticles Research*. Volume 16, pp. 2362–2372

Khalil, M., Liu, N., Lee, R.L., 2017. Catalytic Aquathermolysis of Heavy Crude Oil using Surface-modified Hematite Nanoparticles. *Industrial Engineering & Chemistry Research*, Volume 56, pp. 4572–4579

Kim, E.H., Anh, Y., Lee, H.S., 2007. Biomedical Applications of Superparamagnetic Iron Oxide Nanoparticles Encapsulated within Chitosan. *Journal of Alloys and Compounds*, Volume 434, pp. 633–636

Kulkarni, S.S., Lokhande, C.D., 2003. Structural, Optical, Electrical and Dielectrical Properties of Electrosynthesized Nanocrystalline Iron Oxide Thin Films. *Material Chemistry and Physics*, Volume 82, pp. 151–156

Lee, M.A., Park, B.J., Chin, I., Choi, H.J., 2009. Polymer Modified Hematite Nanoparticles for Electrophoretic Display. *Journal of Electroceramics*, Volume 23, pp. 474–477

Lu, B., Li, P., Liu, H., Zhao, L., Wei, Y., 2012. Synthesis of Hexagonal Pyramidal Columnar Hematite Particles by a Two-step Solution Route and their Characterization. *Powder Technology*, Volume 215–216, pp. 132–136

Pinkas, J., Reichlova, V., Zboril, R., Moravec, Z., Bezdicka, P., Matejkova, J., 2008. Sonochemical Synthesis of Amorphous Nanoscopic Iron (III) Oxide from $Fe(acac)_3$. *Ultrasonics Sonochemistry*, Volume 15, pp. 257–264

Rendon, J.L., Serna, C.J., 1981. IR Spectra of Powder Hematite: Effects of Particles Size and Shape. *Clays Minerals*, Volume 16, pp. 375–381

Schmidt, H., 2001. Nanoparticles by Chemical Synthesis, Processing to Materials and Innovative Applications. *Applied Organometallic Chemistry*, Volume 15, pp. 331–343

Sha, G., Wang, T., Xiao, J., Liang, C., 2004. A Mild Solvothermal Route to α-Fe_2O_3 Nanoparticles. *Material Research Bulletin*, Volume 39, pp. 1917–1921

Suslick, K.S., 1998. *Sonochemistry, in Kirk-Othmer Encyclopedia of Chemical Technology* (4th. Ed.). John Wiley & Sons: New York., pp. 517–541

Tadić, M., Čitaković, N., Panjan, M., Stojanović, Z., Marković, D., 2011. Synthesis, Morphology, Microstructure and Magnetic Properties of Hematite Submicron Particles. *Journal of Alloy and Compounds*, Volume 509, pp. 7639–7644

Vijaykumar, R., Koltypin, Y., Xu, X.N., Yeshurun, Y., Gedanken, A., Felner, I., 2001. Fabrication of Magentite Nanorods by Ultrasound Irradiation. *Journal of Applied Physics*, Volume 89, pp. 6324–6328

Wang, X.K., Chen, G.H., Guo, W.L., 2003. Sonochemical Degradation of Kinetics of Methyl Violet in Aqueous Solutions. *Molecules*, Volume 8, pp. 40–44